

CALCULATION OF HEATING RATE IN THE ANTARCTIC STRATOSPHERE IN 1985 USING SAGE II DATA

Hideharu AKIYOSHI¹, Motowo FUJIWARA² and Michiya URYU¹

¹*Department of Physics, Faculty of Science, Kyushu University,
10-1, Hakozaki 6-chome, Higashi-ku, Fukuoka 812*

²*Department of Applied Physics, Faculty of Science, Fukuoka University,
19-1, Nanakuma 8-chome, Minami-ku, Fukuoka 814-01*

Abstract: The radiative heating effects due to molecules and aerosols over Antarctica during September–October 1985 have been examined, by using a detailed radiative transfer scheme and SAGE II data. In the calculation of radiative transfer, we have considered the absorption of solar radiation, the atmospheric thermal emission and absorption, Rayleigh and Mie scatterings, and the surface scattering effects. The results show that the heating rate in the Antarctic stratosphere during that period is too small to cause effective upward motions, even if aerosol heating is included.

1. Introduction

The Antarctic ozone hole phenomenon has been attracting much attention of many scientists over the world. The preliminary results of the recent observations of ozone and other chemical species over Antarctica are favorable to the idea that chlorine chemistry is a primary cause of the ozone hole (AIKIN, 1988; LEVI, 1988). But there still remain some phenomena which cannot be explained by the chemistry alone, for example, the extreme decrease of the total ozone (25 D.U.) over an area of about 3×10^6 km² in a day (AAOE Fact Sheet, 1987). The mechanism of the depletion of the Antarctic ozone has not yet been fully understood. Clearly, it is crucial to understand the role of some dynamical processes in the Antarctic ozone hole phenomenon (ROSENFELD and SCHOEBERL, 1986).

TUNG *et al.* (1986) suggested that a sudden increase in the absorption of the solar radiation due to O₃ may cause transient upward motions in the Antarctic spring, so that, upwelling ozone poor air in the troposphere may cause the depletion of ozone in the stratosphere. However, SHI *et al.* (1986) pointed out, through their calculation of radiative transfer including infrared emission and absorption, that an upward motion in spring is questionable, unless some other heat source, for example, the stratospheric aerosols from El Chichon Volcano is taken into account. Although the amount of aerosols from the eruption of El Chichon has been decreasing over Antarctica since the winter of 1983 (MCCORMICK and TREPTE, 1987), it will be meaningful to make a correct estimation of the heating effects of the atmospheric aerosols with detailed calculations of radiative transfer, in order to elucidate the dynamical effects on the depletion of ozone in Antarctica.

In the following section, the scheme of the calculations is described. In section

3, we show the heating rates calculated without or with the radiative effects of the stratospheric aerosols. Then, in Section 4, we briefly discuss the possibility of transient upward air motions in the Antarctic spring.

2. Calculations of the Radiative Transfer

2.1. Atmospheric model

We have divided the inhomogeneous atmosphere (from the ground surface to 55 km) into 40 homogeneous layers. The interval of separation is 10 mb from the surface to 16 km, and above 16 km it is a little bit arbitrary. In order to estimate the thermal emission and absorption, and the absorption of solar radiation by the atmosphere above 55 km, we have assumed one homogeneous layer with thickness of the scale-height at the altitude of 55 km as an uppermost boundary. The pressure and temperature of each layer have been interpolated from NOAA data, and the densities of water vapor and ozone have been interpolated from SAGE II data. The mixing ratio of CO₂ was assumed to be constant, 316.5 ppmv, all through the atmosphere.

2.2. Solar spectral region (0.2–4.7 μm)

Absorption bands

The solar spectral region has been divided into 53 subregions of unequal widths, considering the solar spectrum and the absorption bands of H₂O, O₃, CO₂ and O₂ as described below.

O₃: We have used the absorption cross-section data of Hartley, Huggins and Chappius bands taken from WMO Report (1986).

H₂O: The fractional absorptions of the following bands have been considered: 0.94 μm , 1.1 μm , 1.38 μm , 1.87 μm , 2.7 μm , and 3.2 μm bands. The absorption cross-section of each band has been calculated by the exponential fit formulation by LIU and SASAMORI (1975).

CO₂: 1.4 μm , 1.6 μm , 2.0 μm , 2.7 μm , and 4.3 μm bands have been considered. The fractional absorption of each band has been derived from the empirical formula by HOWARD *et al.* (1956).

O₂: We have considered only 0.76 μm band, and used the integrated absorption coefficient by HOUGHTON (1963).

Effects of scattering and absorption due to the aerosols

The scattering and absorption cross-sections of aerosols in the solar spectral region have been estimated by using the Mie theory (DEIRMENDJIAN, 1969). The size distribution of aerosols has been assumed to be of log-normal type with a mean radius (r_m) of 0.1 μm . Moreover, its standard deviation (σ) has been adjusted so that a wavelength dependence of the calculated extinction fits to that of the extinction in the Antarctic stratosphere observed by SAGE II (Fig. 1 and Fig. 2). In this calculation, we have assumed that the imaginary part of refractive index is 0.001 in the visible region, considering that the atmospheric aerosols may contain a small amount of impurities such as volcanic ashes. The vertical distribution of the number density of aerosols has been adjusted so that the calculated extinction cross-section

Fig. 1. The dependence of the calculated extinction cross-section of aerosols with size distributions on wavelength. The size distributions were assumed to be log-normal function with a mean radius $r_m = 0.1 \mu\text{m}$, in which the standard deviation σ is variable between 1.86 and 2.3 depending on the extinction data.

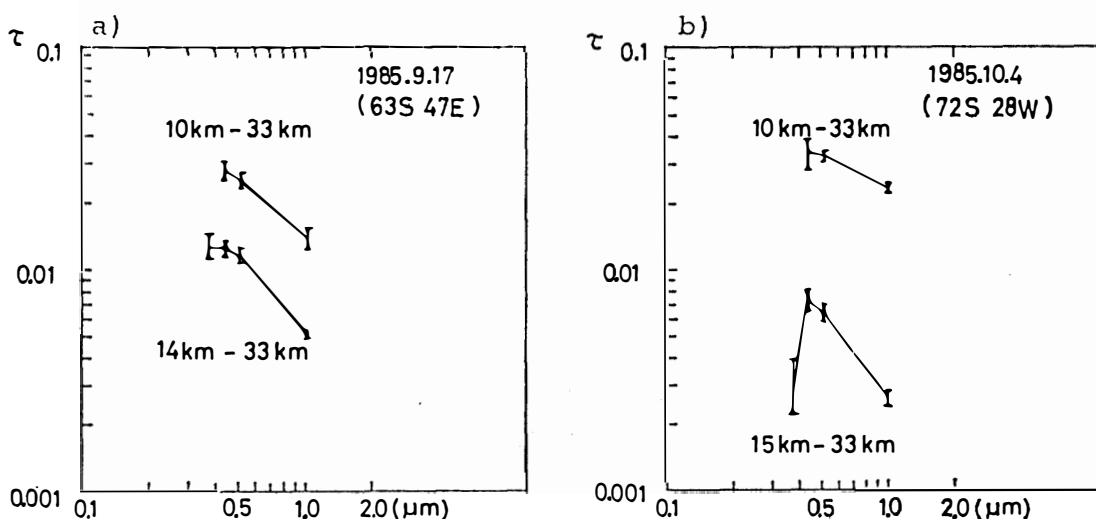
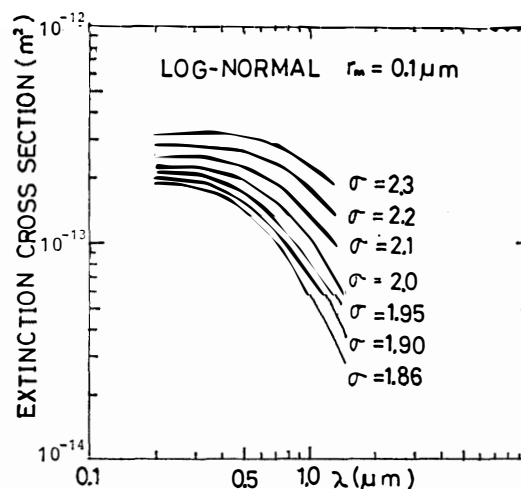


Fig. 2. The observed optical depths of the atmospheric aerosols at 3 or 4 wavelength by SAGE II. Error bars are also shown.

at $0.525 \mu\text{m}$ agrees with that of SAGE II data.

The single scattering albedo and the normalized phase function of the L th layer can be written, respectively, as follows:

$$\langle L \rangle \tilde{\omega}_{0, R+M}(\lambda) = \frac{\langle L \rangle \Delta\tau_R(\lambda) + \langle L \rangle \Delta\tau_{M, s}(\lambda)}{\langle L \rangle \Delta\tau_R(\lambda) + \langle L \rangle \Delta\tau_a(\lambda) + \langle L \rangle \Delta\tau_{M, s}(\lambda) + \langle L \rangle \Delta\tau_{M, a}(\lambda)},$$

$$\langle L \rangle P_{R+M}(\mu, \lambda) = \frac{\langle L \rangle \Delta\tau_R(\lambda) \cdot \langle L \rangle P_R(\mu, \lambda) + \langle L \rangle \Delta\tau_{M, s}(\lambda) \cdot \langle L \rangle P_M(\mu, \lambda)}{\langle L \rangle \Delta\tau_R(\lambda) + \langle L \rangle \Delta\tau_{M, s}(\lambda)},$$

where

μ : cosine of the solar zenith angle,

$\langle L \rangle P_R(\mu, \lambda)$: phase function for the molecules in the L th layer at wavelength λ ,

$\langle L \rangle P_M(\mu, \lambda)$: phase function for the aerosols in the L th layer at wavelength λ ,

$\langle L \rangle \Delta\tau_R(\lambda)$: Rayleigh scattering optical depth of the L th layer at wavelength λ ,

$\langle L \rangle \Delta\tau_a(\lambda)$: optical depth of the absorption of the L th layer at wavelength λ due to H_2O , CO_2 , O_3 and O_2 ,

${}^{(L)}\Delta\tau_{\mathbf{M},\mathbf{s}}(\lambda)$: optical depth of the scattering of the L th layer at wavelength λ due to aerosols,

${}^{(L)}\Delta\tau_{\mathbf{M},\mathbf{a}}(\lambda)$: optical depth of the absorption of the L th layer at wavelength λ due to aerosols.

Then, asymmetric factors of the L th layer at wavelength λ ${}^{(L)}g_{\mathbf{R}+\mathbf{M}}(\lambda)$, and ${}^{(L)}\beta_{0,\mathbf{R}+\mathbf{M}}(\lambda)$ are written as follows:

$$g_{\mathbf{R}+\mathbf{M}}(\lambda) = \frac{\Delta\tau_{\mathbf{M},\mathbf{s}}(\lambda)}{\Delta\tau_{\mathbf{R}}(\lambda) + \tilde{\omega}_{0,\mathbf{M}}(\lambda) \cdot \Delta\tau_{\mathbf{M},\mathbf{s}}(\lambda)} \cdot \frac{\tilde{\omega}_{1,\mathbf{M}}(\lambda)}{3}$$

$$\beta_{0,\mathbf{R}+\mathbf{M}}(\lambda) = \frac{\frac{1}{2} \Delta\tau_{\mathbf{R}}(\lambda) + \frac{1}{2} \Delta\tau_{\mathbf{M},\mathbf{s}}(\lambda) \cdot \int_{-1}^0 P_{\mathbf{M}}(\mu) d\mu}{\Delta\tau_{\mathbf{R}}(\lambda) + \tilde{\omega}_{0,\mathbf{M}}(\lambda) \cdot \Delta\tau_{\mathbf{M},\mathbf{s}}(\lambda)},$$

where $\tilde{\omega}_{1,\mathbf{M}} = (3/2) \int_{-1}^{+1} P_{\mathbf{M}}(\mu) \cdot \mu \cdot d\mu$, and the symbol “ ${}^{(L)}$ ” is omitted.

Numerical scheme of radiative transfer including scattering and absorption

In order to consider the effects of the scattering and absorption by air molecules, aerosols and the surface, we have used a two-stream approximation (modified Eddington-delta function hybrid method by MEADOR and WEAVER (1980)). Then, we can obtain the upward and downward diffusive flux as a function of the altitude, wavelength and solar zenith angle as follows:

$${}^{(L)}F^+_{\text{DIFF}}(\tau_L) = {}^{(L)}A \cdot \exp[{}^{(L)}k \cdot \tau_L] + {}^{(L)}B \cdot \exp[-{}^{(L)}k \cdot \tau_L]$$

$$+ \frac{{}^{(L)}\tilde{\omega}_0 \cdot \mu_0 \pi F_0 ({}^{(L)}\gamma_3 - {}^{(L)}\alpha_2 \cdot \mu_0)}{1 - {}^{(L)}k^2 \cdot \mu_0^2} \cdot \exp[-\tau_L/\mu_0]$$

for upward diffusive flux, and

$${}^{(L)}F^-_{\text{DIFF}}(\tau_L) = -\frac{{}^{(L)}k - {}^{(L)}\gamma_1}{{}^{(L)}\gamma_2} \cdot {}^{(L)}A \cdot \exp[{}^{(L)}k \cdot \tau_L] + \frac{{}^{(L)}k + {}^{(L)}\gamma_1}{{}^{(L)}\gamma_2} \cdot {}^{(L)}B \cdot \exp[-{}^{(L)}k \cdot \tau_L]$$

$$- \frac{{}^{(L)}\tilde{\omega}_0 \cdot \mu_0 \pi F_0 ({}^{(L)}\gamma_4 + {}^{(L)}\alpha_1 \cdot \mu_0)}{1 - {}^{(L)}k^2 \cdot \mu_0^2} \cdot \exp[-\tau_L/\mu_0]$$

for downward diffusive flux, where

τ_L : optical depth from the top of the atmosphere to the lower boundary of the L th layer (Fig. 3),

${}^{(L)}A, {}^{(L)}B$: constants determined by boundary conditions.

Other constants in the equations, $k, \gamma_1, \gamma_2, \gamma_3, \gamma_4, \alpha_1$ and α_2 follow MEADOR and WEAVER (1980). The boundary conditions have been given as follows (see Fig. 3);

- 1) No downward diffusive flux at the top of the atmosphere.
- 2) The upward and downward flux have to be continuous at the boundary of each homogeneous layer.
- 3) The ground is assumed to be an isotropic reflector with an albedo of 0.5, independent of the wavelength in the solar spectral region.

We have calculated the inverse matrix by Crout method to solve 82 linear equa-

$$F^+_{DIFF}(\tau) = A \cdot \exp(k\tau) + B \cdot \exp(-k\tau) + \frac{\pi F_0 \omega_0 \mu_0 (\gamma_2 - \mu_0 \alpha_2)}{1 - \mu_0^2 k^2} \cdot \exp(-\tau / \mu_0)$$

$$F^-_{DIFF}(\tau) = -\frac{k - \gamma_1}{\gamma_2} \cdot A \cdot \exp(k\tau) + \frac{k + \gamma_1}{\gamma_2} \cdot B \cdot \exp(-k\tau) - \frac{\pi F_0 \omega_0 \mu_0 (\gamma_1 + \mu_0 \alpha_1)}{1 - \mu_0^2 k^2} \cdot \exp(-\tau / \mu_0)$$

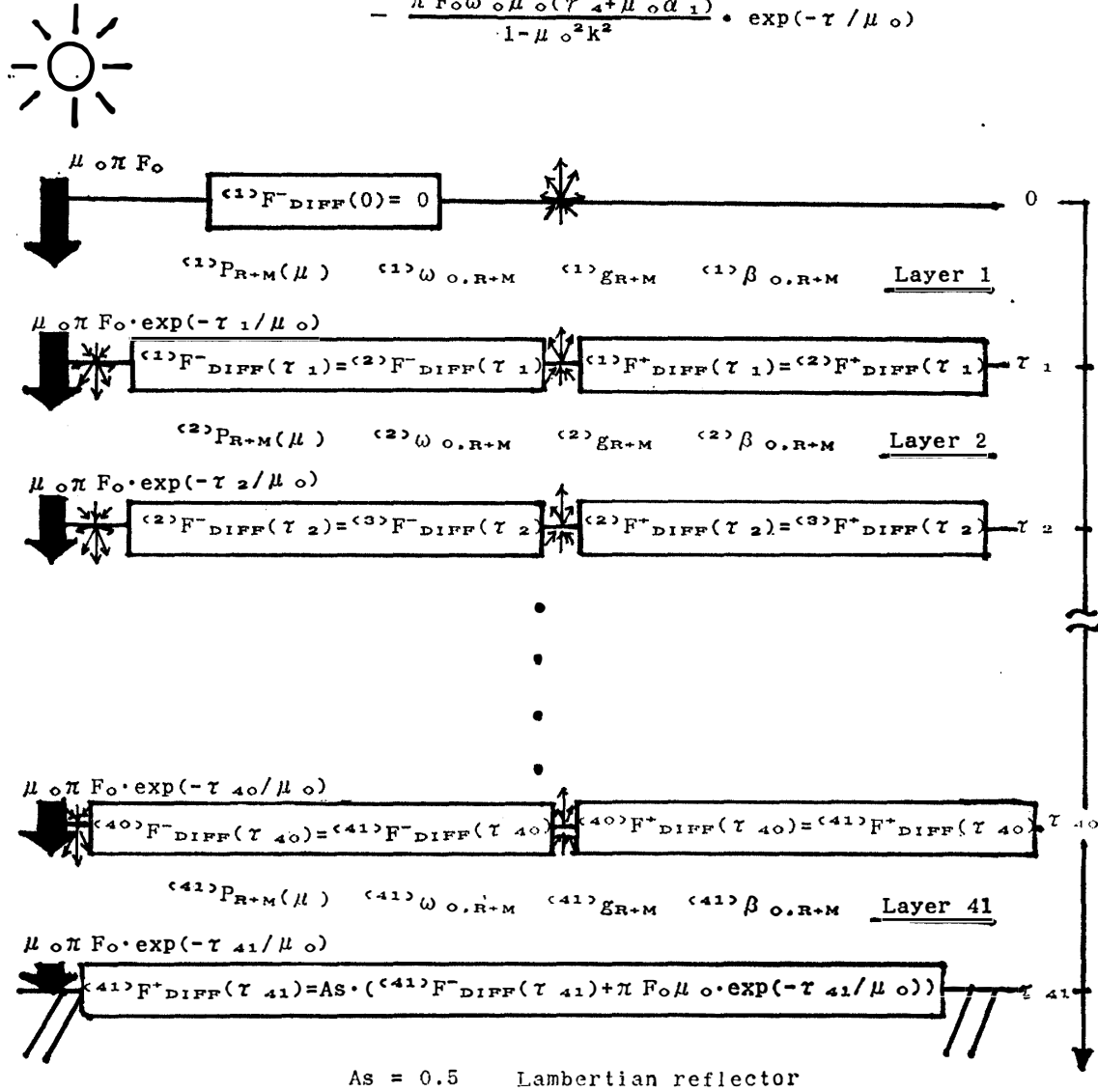


Fig. 3. The atmospheric model used in our radiative calculation. Solar flux at the top of the atmosphere is indicated by " $\mu_0 \pi F_0$ ". The direct component of the flux is shown on the left side, and the upward and downward diffusive components of the flux at the optical depth τ are expressed in the upper part of this figure. The equations in rectangular frames indicate boundary conditions for the diffusive flux. The ground surface is assumed to be a Lambertian reflector with albedo 0.5.

tions numerically. However, in the case of large τ_L at low altitudes, the difference between $\exp(^{(L)}k \cdot \tau_L)$ and $\exp(-^{(L)}k \cdot \tau_L)$ values increases, making the coefficient matrix to be singular. So, we have rewritten $^{(L)}A \cdot \exp(^{(L)}k \cdot \tau_L)$ and $^{(L)}B \cdot \exp(-^{(L)}k \cdot \tau_L)$ terms respectively, as follows:

$$\begin{aligned} ^{(L)}A \cdot \exp(^{(L)}k \cdot \tau_L) &= ^{(L)}A \cdot \exp(^{(L)}k \cdot \tau_{L-1}) \cdot \exp(^{(L)}k(\tau_L - \tau_{L-1})) \\ &= ^{(L)}A' \cdot \exp(^{(L)}k(\tau_L - \tau_{L-1})), \\ ^{(L)}B \cdot \exp(-^{(L)}k \cdot \tau_L) &= ^{(L)}B \cdot \exp(-^{(L)}k \cdot \tau_{L-1}) \cdot \exp(-^{(L)}k(\tau_L - \tau_{L-1})) \\ &= ^{(L)}B' \cdot \exp(-^{(L)}k(\tau_L - \tau_{L-1})). \end{aligned}$$

We have calculated $^{(L)}A'$ and $^{(L)}B'$ instead of $^{(L)}A$ and $^{(L)}B$.

We have now obtained the monochromatic diffusive upward and downward fluxes. Since it is easy to evaluate the direct component of the fluxes, we can calculate the solar heating rate of each layer, by integrating monochromatic fluxes over the full wavelength region of the solar spectrum.

2.3. Thermal region (4.5–250 μm)

We have considered the absorption and emission due to H_2O rotational band, H_2O 6.3 μm band, CO_2 15 μm band, and O_3 9.6 μm band. The spectral region has been divided into 31 subregions, taking these absorption bands into account. We have used Goody's random model, and Curtis-Godson's two-parameter approximation to derive an averaged transmission in the subregions (GOODY, 1964; GOLDMAN and KYLE, 1968; ROEWE and LIU, 1978).

The absorption cross-section of aerosols in the infrared region has been calculated by the Mie theory in the same way as in the solar spectral region. We have assumed that the atmospheric aerosols are 75% H_2SO_4 droplets in this calculation, and used the data of the refractive index of 75% H_2SO_4 (PALMER and WILLIAMS, 1975). The scattering due to aerosols have been ignored in the infrared region.

Using the transmission between τ_L and τ' , in each subregion, we can evaluate the monochromatic upward and downward fluxes in the infrared region:

$$\begin{aligned} F_{\Delta\lambda}^+(\tau_L)_{\text{INFRA}} &= \pi \bar{B}_{\Delta\lambda}(\bar{T}_{\text{sfc}}) \cdot \bar{T}r_{\Delta\lambda}(\tau_L, \tau_{\text{sfc}}) + \int_{\bar{T}r_{\Delta\lambda}(\tau_L, \tau_{\text{sfc}})}^1 \pi \bar{B}_{\Delta\lambda}(T(\tau')) \cdot d\bar{T}r_{\Delta\lambda}(\tau_L, \tau'), \\ F_{\Delta\lambda}^-(\tau_L)_{\text{INFRA}} &= \int_{\bar{T}r_{\Delta\lambda}(\tau_L, 0)}^1 \pi \bar{B}_{\Delta\lambda}(T(\tau')) \cdot d\bar{T}r_{\Delta\lambda}(\tau_L, \tau'), \end{aligned}$$

where

$\bar{T}r_{\Delta\lambda}(\tau_L, \tau')$: transmission between τ_L and τ' ,

$T(\tau')$: temperature at τ' ,

T_{sfc} : temperature at the ground surface,

τ_{sfc} : optical depth from the top of the atmosphere to the ground surface ($=\tau_{41}$),

$\bar{B}(T(\tau'))$: Planck function at the temperature T in the spectral interval $\Delta\lambda$.

Then, the total cooling rate or heating rate in the infrared region has been obtained, by integrating them over the full wavelength range.

3. Results

Figure 4 shows the vertical distribution of the day-averaged solar heating rate, infrared cooling rate, and net heating rate on several days in September and October, 1985. In these figures, the radiative effects of stratospheric aerosols are excluded. These calculations are based on SAGE II data. It seems that there is no significant radiative diabatic heating in this period in the lower stratosphere without aerosols.

Figure 5 also shows the vertical distributions of the heating rate without aerosols on the same days as in Fig. 4, but in this calculation, we have used the O_3 data on March 5, 1985 ($69^\circ S$) instead of the O_3 data on the days shown. It is noted

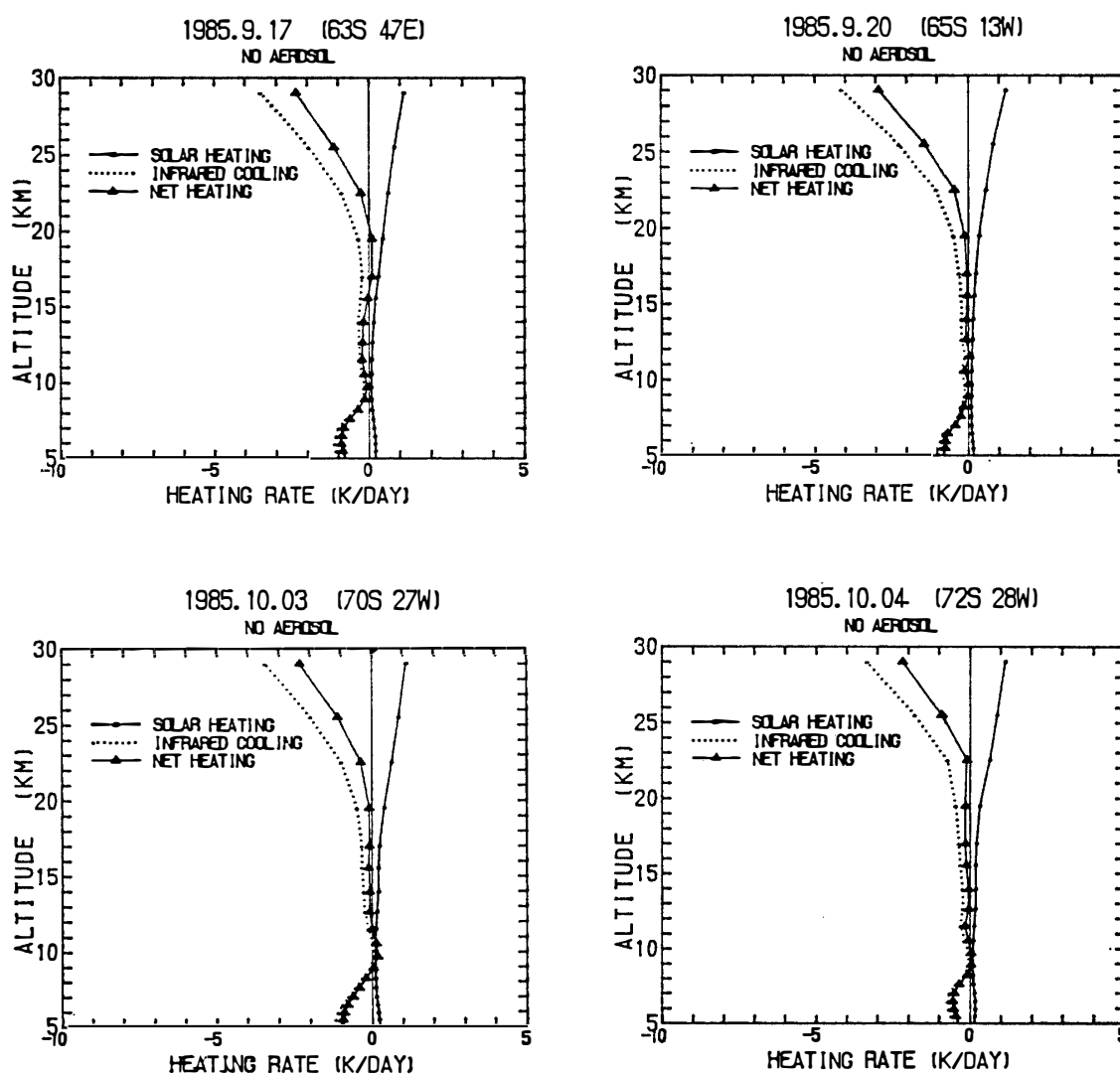


Fig. 4. Day-averaged heating rate ignoring aerosols in several days in September–October, 1985. Solid line, dotted line, and triangle show solar heating, thermal cooling, and net heating, respectively. These calculations are based on SAGE II data.

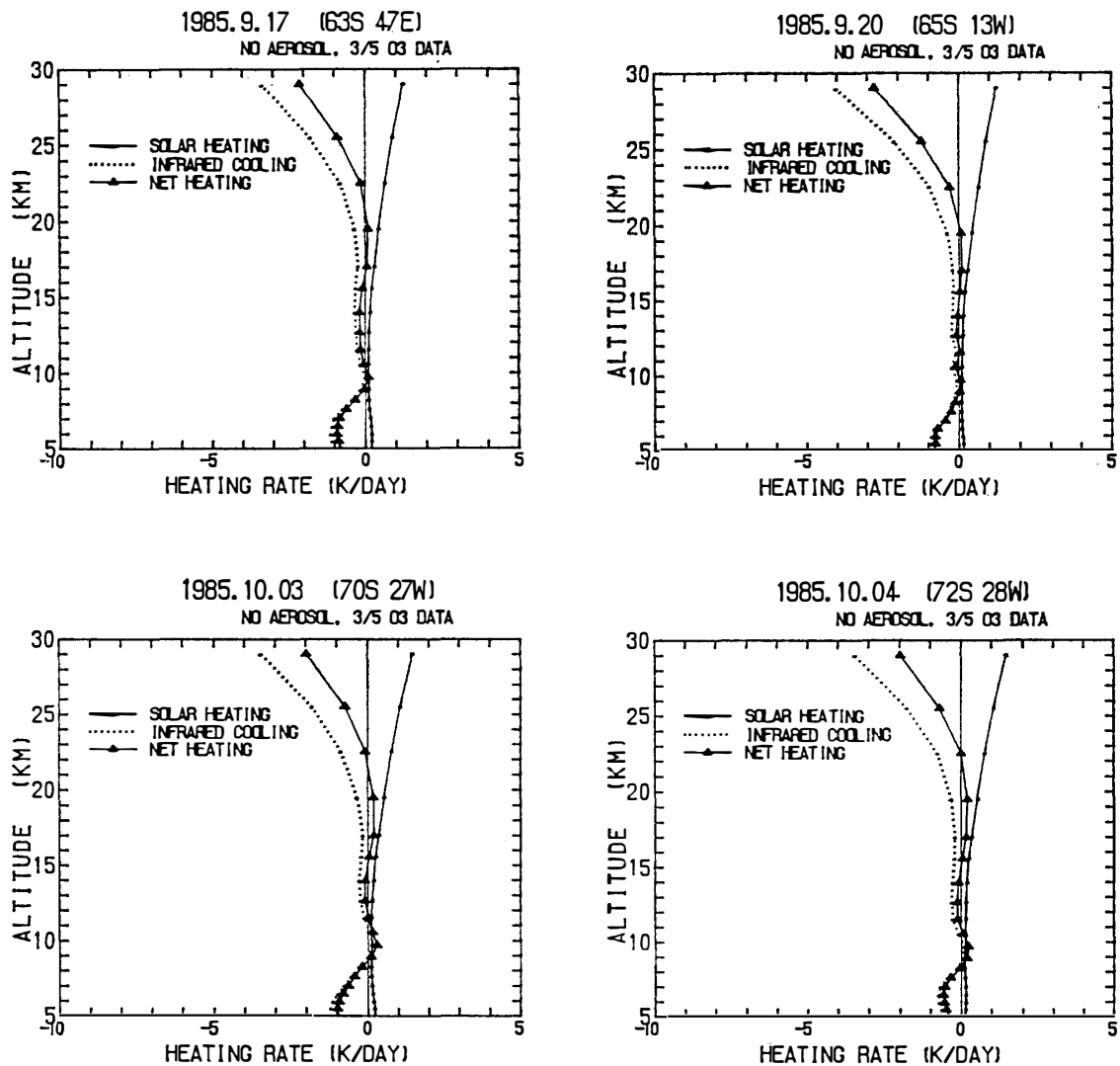


Fig. 5. Same as Fig. 4, except that the zonal mean data of O_3 at $69^\circ S$ on March 5, 1985 were used in the calculation instead of the O_3 data on that day.

that the column abundance of O_3 on May 5, 1985 was almost equal to that during the polar night. It seems impossible to cause upward motions without aerosols during the Antarctic spring, even if we take account of a possible upper limit of the heating rate. These results are almost the same as those of AKIYOSHI *et al.* (1988).

We have also calculated the vertical distribution of the additional heating rate due to aerosols, that is, the difference between the heating rate including the radiative effects from aerosols and the heating rate without them, during mid September–mid October. (See Fig. 3, AKIYOSHI *et al.* (1988)). The result shows that the additional heating rates in the Antarctic spring, 1985 are smaller than 0.1 K/day, although we have chosen the data inside the polar vortex.

4. Discussion

The uncertainty in the composition of the atmospheric aerosols prevents us from an accurate evaluation of the absorption efficiency for the solar and thermal radiation. For example, volcanic ashes can remarkably increase the absorption of visible light due to the aerosols. On the other hand, a change in the sulfuric acid concentration within the aerosols affects the absorption mainly in the infrared region.

We have assumed that the stratospheric aerosols are 75%-H₂SO₄ droplets, and we have used the refractive index value of 75%-H₂SO₄ aerosols. Although H₂SO₄ solution has a very small imaginary part of the refractive index in the visible region, we have assumed that the imaginary part is 0.001 in this region, considering that the aerosols may contain some impurities such as volcanic ashes. We believe that these assumptions for the optical properties of aerosols and the assumption for size distribution will lead to somewhat magnified heating rates due to the Antarctic stratospheric aerosols in 1985 (see Discussion and Conclusions 1)–5), AKIYOSHI *et al.*, 1988).

We have assumed a constant value, 0.5 of surface albedo in the solar spectral region. This value may be a little smaller for the Antarctic ground surface. However, a sensitivity test with albedo 1.0 gives only 20% increase in the additional heating in the solar spectral region and 10% increase in the total additional heating rate. This is because of a low solar elevation.

According to our calculations of the heating rate, the atmospheric heatings due to the stratospheric aerosols and molecules seem to be too small to cause any effective upward motion in the Antarctic spring, although most of parameters used in this calculation seem to contribute to magnify the heating effects of the atmospheric aerosols. But yet, we are not able to answer clearly whether or not an effective upward motion will be resulted, because the possible effects from atmospheric dynamics are not included in our model.

5. Concluding Remarks

We have examined, through detailed calculations of the radiative transfer in the atmosphere, whether any net radiative heating could occur over the Antarctica in September–October, 1985. The results show that the atmospheric heatings due to the stratospheric molecules and aerosols are too small to cause any upward motion, and hence, to cause the ozone depletion due to this mechanism in this period. However, we cannot yet conclude definitely whether or not any upward motion occur, because we have not yet taken account of dynamics in our model.

Acknowledgments

The authors would like to thank Dr. M. P. McCORMICK for supplying us with SAGE II data. We are also grateful to Mr. CHUBACHI, and Drs. M. TAKAHASHI and M. HIRONO for many helpful discussions, and Dr. M. TAKEFU for his guidance in the use of MS-DOS.

References

- AIKIN, A. C. (1988): Polar Ozone Workshop—Abstracts—May 1988. Washington, D.C., NASA Conf. Publ., NASA CP-10014, 329 p.
- AIRBORNE ANTARCTIC OZONE EXPERIMENT (1987): Fact Sheet; Initial findings from Punta Arenas, Chile, September 30, 1987. NASA, NOAA, CMA and NSF.
- AKIYOSHI, H., FUJIWARA, M. and URYU, M. (1988): Radiative aspects of the Antarctic ozone hole in 1985. *Geophys. Res. Lett.*, **15**, 919–922.
- DEIRMENDJIAN, D. (1969): *Electromagnetic Scattering on Spherical Polydispersions*. New York, Elsevier, 290 p.
- GOODY, R. M. (1964): *Atmospheric Radiation. I. Theoretical Basis*. London, Oxford Univ. Press, 436 p.
- GOLDMAN, A. and KYLE, T. G. (1968): A comparison between statistical model and line by line calculation with application to the 9.6- μ ozone and the 2,7- μ water vapor bands. *Appl. Opt.*, **7**, 1167–1177.
- HOUGHTON, J. T. (1963): The absorption of solar infra-red radiation by the lower stratosphere. *Quart. J. R. Meteorol. Soc.*, **89**, 319–331.
- HOWARD, J. N., BURCH, D. E. and WILLIAMS, D. (1956): Infrared transmission of synthetic atmospheres, Parts I–V. *J. Opt. Soc. Am.*, **46**, 186–190, 237–241, 242–245, 334–338, 452–455.
- LEVI, B. G. (1988): Ozone depletion at the poles; The hole story emerges. *Phys. Today*, **41**, 17–21.
- LIU, K. N. and SASAMORI, T. (1975): On the transfer of solar radiation in aerosol atmospheres. *J. Atmos. Sci.*, **32**, 2166–2177.
- MCCORMICK, M. P. and TREPTE, C. R. (1987): Polar stratospheric optical depth observed between 1978 and 1985. *J. Geophys. Res.*, **92**, 4297–4306.
- MEADOR, W. E. and WEAVER, W. R. (1980): Two-stream approximations to radiative transfer in planetary atmospheres; A unified description of existing methods and a new improvement. *J. Atmos. Sci.*, **37**, 630–643.
- PALMER, K. F. and WILLIAMS, D. (1975): Optical constants of sulfuric acid; Application to the clouds of Venus? *Appl. Opt.*, **14**, 208–219.
- ROEWE, D. and LIU, K. N. (1978): Influence of cirrus clouds on the infrared cooling rate in the troposphere and lower stratosphere. *J. Appl. Meteorol.*, **17**, 92–106.
- ROSENFELD, J. E. and SCHOEBERL, M. R. (1986): A computation of stratospheric heating rates and the diabatic circulation for the Antarctic spring. *Geophys. Res. Lett.*, **13**, 1339–1342.
- SHI, G. Y., WANG, W. C., KO, M. K. W. and TANAKA, M. (1986): Radiative heating due to stratospheric aerosols over Antarctica. *Geophys. Res. Lett.*, **13**, 1335–1338.
- TUNG, K. K., KO, M. K. W., RODRIGUEZ, J. M. and SZE, N. D. (1986): Are Antarctic ozone variations a manifestation of dynamics or chemistry? *Nature*, **322**, 811–814.
- WORLD METEOROLOGICAL ORGANIZATION (1986): *Atmospheric ozone 1985; Assessment of our understanding of the processes controlling its present distribution and change*. WMO Report, **16**, Global Ozone Research and Monitoring Project. Geneva, WMO.

(Received May 1, 1988; Revised manuscript received January 27, 1989)